Crack characterization using guided circumferential waves

Christine Valle
Department of Mechanical Engineering, University of Maine, Orono, Maine 04469-5711

Marc Niethammer
School of Civil and Environmental Engineering, Georgia Institute of Technology, Atlanta, Georgia 30332-0355

Jianmin Qu
G. W. W. School of Mechanical Engineering, Georgia Institute of Technology, Atlanta, Georgia 30332-0405

Laurence J. Jacobs
School of Civil and Environmental Engineering, Georgia Institute of Technology, Atlanta, Georgia 30332-0355

(Received 1 August 2000; revised 15 March 2001; accepted 14 May 2001)

This paper examines the propagation of guided circumferential waves in a hollow isotropic cylinder that contains a crack, with the goal of using these guided waves to both locate and size the crack. The crack is sized using a modified Auld's formula, which relates the crack's length to a reflected energy coefficient. The crack is then located by operating on the backscattered signal with a time-frequency digital signal processing (DSP) technique, and then comparing these results to those obtained if the cylinder is perfect. The guided circumferential waves are generated with a commercial finite element method (FEM) code. One objective of this work is to demonstrate the effectiveness of using sophisticated DSP techniques to describe the effect of scattering on dispersive waves, showing it is possible to characterize cracks systematically and accurately by quantifying this scattering effect. The results show that the need for high frequency signals to detect small cracks is significantly decreased by using these techniques. © *2001 Acoustical Society of America.* [DOI: 10.1121/1.1385899]

PACS numbers: 43.20.Fn, 43.20.Mv [DEC]

I. INTRODUCTION

It is well known that fatigue cracks can initiate and grow in the radial direction of an annular structure that is subjected to a large number of fatigue cycles. These annular structures are used extensively in a variety of industrial applications, such as the aerospace, oil and nuclear industries. A quantitative and systematic inspection methodology is needed to detect and characterize these cracks, before a catastrophic structural failure occurs.

Ultrasonic testing is a candidate nondestructive evaluation (NDE) methodology for this application. Unfortunately, traditional ultrasonic techniques (such as pulse-echo) are ineffective in this application because of problems associated with curvature and accessibility difficulties. Guided ultrasonic waves, i.e., waves that propagate in the direction of the layer while behaving as standing waves through the thickness of the layer, are a potential alternative. Nagy *et al.*[1] recently proposed using guided ultrasonic waves that propagate in the circumferential direction to detect radial cracks in weep holes of airframes.

The main advantage in using guided ultrasonic waves is that they can interrogate the entire specimen, including inaccessible portions. Unfortunately, the detected ultrasonic signals are very complicated, causing difficulties in signal interpretation. Previous researchers have studied guided waves in plates[2] and cylinders.[3] For example, Alleyne and Cawley[3] examine cylindrical waves that propagate down the axis of the cylinder *but remain standing in its circumferential direction* to detect cracks in long thin pipes. [That is, the expressions for the field quantities contain terms such as $\cos(n\theta)$ or $\sin(n\theta)$, where θ is the usual polar angle (see Fig. 1) and n is an integer. Thus quantities such as velocities or stresses are modulo $[2\pi]$ periodic.] However, these longitudinal waves are not well suited for determining the *radial* location of a crack in a short annular structure. This is especially true for a cylindrical component whose diameter is on the same order of magnitude as its length. Circumferential waves, that is guided waves *that propagate in the circumferential direction of the cylinder*, i.e., in the θ direction (see Fig. 1), are proposed for these applications. Such waves, contrary to the previous case, contain terms such as $e^{ik\theta}$, where θ has the same meaning as previously and k is a **real** number (and not an integer). Thus quantities such as velocities and stresses are not periodic modulo $[2\pi]$. These circumferential waves do not propagate in the z direction (in the axis of the cylinder or along its length). Guided circumferential waves have been studied in Refs. 4 and 5 and were first introduced by Viktorov[6,7] as the natural extension of Lamb waves from a flat plate to a curved plate. Liu and Qu[8] consider the time harmonic analysis of a (perfect) hollow cylinder, while Valle *et al.*[4] examine the time harmonic behavior of a double-layered, hollow cylinder. None of these studies consider transient circumferential waves propagating in a cracked cylindrical component.

This paper examines the propagation of (transient) guided circumferential waves in a metallic (steel) hollow

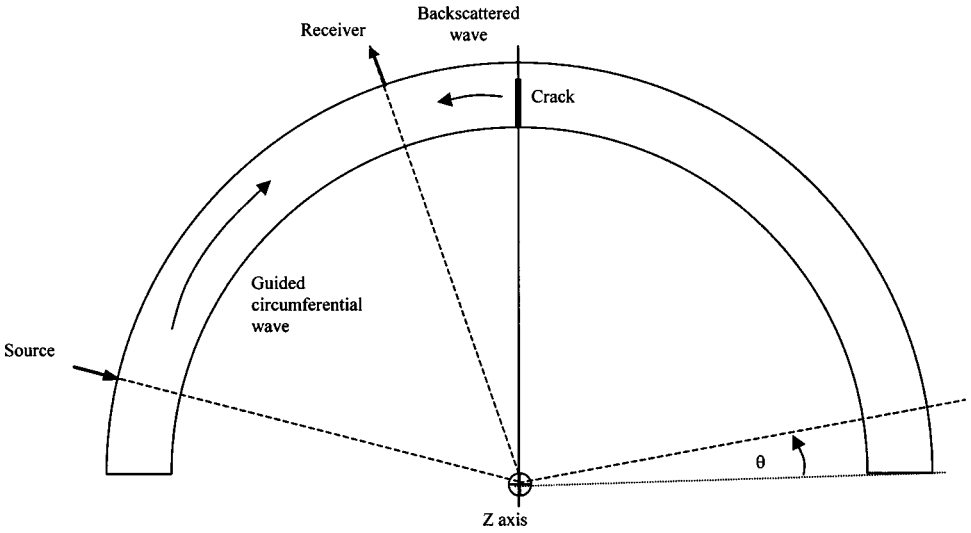

FIG. 1. Specimen geometry, taking advantage of symmetry of hollow cylinder, and simulating laser interrogation with a normal point load/point receiver system for backscattered energy detection.

cylinder that contains a crack, using these guided waves to both locate and size the crack. The crack is sized using a scattering formula first developed by Auld,[9] which is modified in the current work to analyze transient (non-time-harmonic) signals. The crack is then located by operating on the backscattered signal with a time-frequency digital signal processing (DSP) technique, and then comparing these results to those obtained from a perfect cylinder—one without a crack. All the time signals (guided circumferential waves) presented in this work are generated using a commercial FEM code (ABAQUS/Explicit)—except for accuracy checks done by comparing experimental and numerical results. While much fundamental work has been done in the past to develop numerically efficient methods to calculate the transient response of waveguides (both perfect and flawed),[10,11] the FEM was chosen here for its robustness, accuracy and convenience.

It is important to note that no effort is made in this work to selectively restrict the number of guided modes propagating in the cylinder.

One objective of this work is to demonstrate the effectiveness of using sophisticated DSP techniques to describe *guided, broadband, and multi-mode* circumferential waves in imperfect cylinders. Specifically, these DSP techniques are used to examine the effect of scattering on dispersive waves, showing it is possible to characterize cracks systematically and accurately by quantifying this scattering effect.

In this text, the term *wave* designates any ultrasonic signal that propagates into the annular structure under investigation. The term *mode* designates an ultrasonic signal fully represented in a time harmonic fashion by a single curve on the dispersion curves of the structure where the mode propagates (such as, the familiar Lamb modes a_0 and s_0). Therefore, a mode is always a wave, but a wave can consist of multiple modes (since, as an example, the a_0 and s_0 modes can co-exist for a given frequency range).

II. FEM MODEL OF THE SCATTERING OF GUIDED CIRCUMFERENTIAL WAVES CAUSED BY A CRACK

In the past, the computational cost of modeling high-frequency wave propagation problems was prohibitively high. It has been shown recently that the FEM is capable of modeling such problems accurately and efficiently. This computer power increase makes the FEM an excellent method for solving wave propagation problems that are intractable by analytical methods.[12,13]

This numerical study only models a portion (half) of the cylinder, because the signal processing techniques only make use of the backscattered data and thus the whole circumference need not be modeled. The backscattered data will reach the receiver before the transmitted data, and therefore the backscattered data can be windowed out. Also, FE simulations show that most of the signal attenuates by the time it has traveled 360°. Therefore, there is no need to model the complete cylinder. As such this geometry may be thought of as an infinitely long curved plate. ABAQUS/Explicit is used for all numerical calculations. Convergence is reached when the solution obtained is mesh-invariant (the solution remains the same when the mesh size is decreased). As a further check, solutions for the perfect cylinder are compared to the normal modal expansion (NME) calculations of Liu and Qu[14] (see Fig. 2), and to experimentally generated signals (using laser ultrasonics),[5] shown in Fig. 3. The excellent agreement between these solutions confirms the accuracy of these FEM models. A typical half cylinder mesh (the dimensions of the cylinder used in this research are shown in Table I) has 4000 elements (for loads of 0.5 MHz center frequency). This number of elements is obtained by successive refinement of the mesh until mesh invariance is obtained. The element size is 15 times smaller than the wavelength of the (nondispersive) shear wave at the center point of the bandwidth (0.5 MHz) and nearly 7 times smaller at the upper end of the bandwidth (1.5 MHz). While these ratios are low at the higher frequencies, mesh invariance and the numerical validation with Fortran show that they are sufficient for ABAQUS/Explicit.

Each element is a 4-node plain strain continuum element (CPE4R). Such an element provides a second-order interpolation, with reduced integration and hourglass control (hourglassing is a numerical phenomena by which a zero-energy mode propagates through and spoils the solution—see the ABAQUS Theory manual,[15] Sec. 3.1.1, for more details).

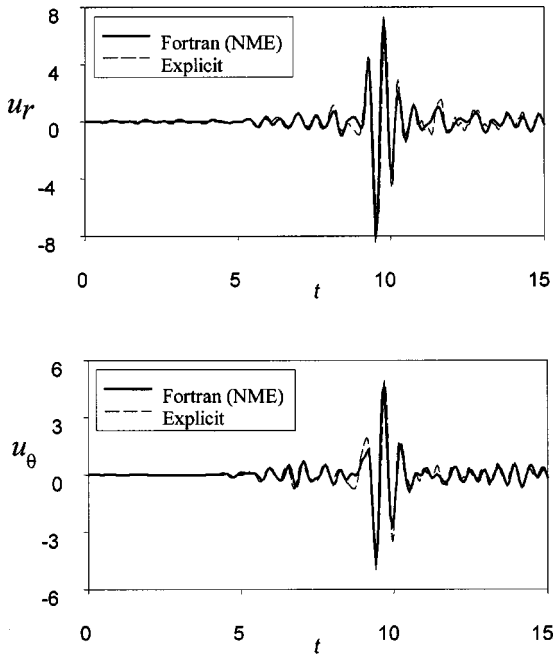

FIG. 2. Comparison between wave forms from Abaqus/Explicit and FORTRAN [normalized units (Ref. 12)].

Each node has 2-degrees of freedom (plane strain assumption).

Cracks in the cylinder are modeled by releasing nodes along the cylinder's wall and are assumed to have perfectly smooth faces, subjected to stress free boundary conditions. Such mesh discontinuities are infinitely thin, are a good representation of a fatigue crack (as opposed to notches), and allow for a variable crack length. In the far field (which is the domain of interest here). For near field calculations, singular elements must be used to accurately capture the singularity at the crack tip. It is important to note that the inverse problem solved in this study does operate under the assumption that the shape of the crack is known *à priori*. In addition, while

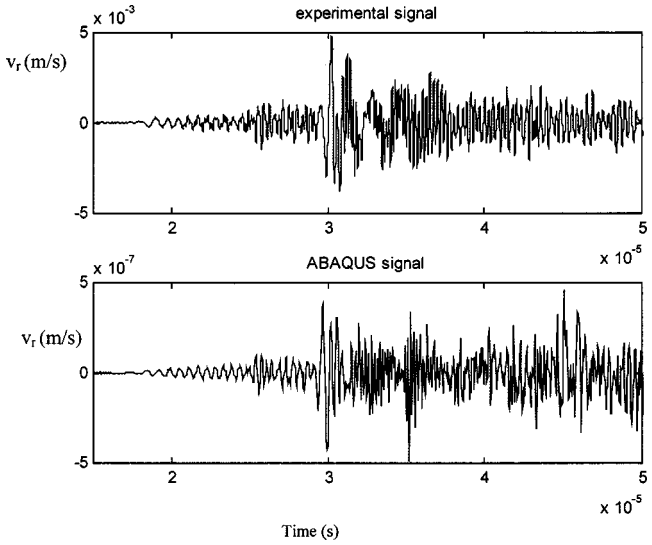

FIG. 3. Comparison between a laser-based experimental signal and the equivalent ABAQUS/Explicit signal.

TABLE I. Material and geometry data for the thin steel annulus.

v	c_T	c_L	a	b	η
0.2817	3120 m/s	5660 m/s	5.08 cm	5.38 cm	0.944 24

crack closure is of clear concern in practical cases, it will not be addressed in this work.

A finer mesh is needed to accurately model cylinders with smaller cracks (i.e., of length smaller than 20% of the wall of the waveguide). Convergence is usually obtained after increasing the number of elements in both the thickness and the waveguide axis directions. Therefore, the computational models presented here can detect cracks of length no smaller than 10% of the wall, that is, no smaller than 0.3 mm for a load with 0.5 MHz center frequency. More powerful computers can capture scattering due to even smaller cracks because they can accurately resolve the bigger meshes needed for loads of higher center frequencies.

The load in all cases is a point load, applied normally to the cylinder's surface. This load has a frequency range of 0.2 to 1.5 MHz, with most of the energy centered near 0.5 MHz. The solution of such a FEM model takes a few minutes on a Pentium III with a 433 MHz clock and 254 MB RAM.

III. AULD's FORMULA

Auld's formula[9,16] is developed using a two transducer, through transmission system applied to the structure to be interrogated. Transducer 1 produces an incident field of power P, and transducer 2 is the receiver [see Figs. 4(a) and (b)]. The ratio of received electrical signal strength, E_{II}, to incident electrical signal strength, E_I, is denoted by Γ. The change in the ratio, $\delta\Gamma$, due to a single scatterer (a crack in this case), is proportional to the reflection coefficient R and is given by Auld's formula:

$$\delta\Gamma = ((E_{II})_{\text{flaw}} - (E_{II})_{\text{noflaw}})/(E_I)_{\text{flaw}}. \tag{1}$$

This formula may be simplified for the case of backscattering, and with the hypothesis that the signals are time harmonic:

$$\delta\Gamma = -\frac{i\omega}{4P}\int_S (\sigma_{kj}^{(2)} u_k^{(1)} - \sigma_{kj}^{(1)} u_k^{(2)}) n_j \, dS, \tag{2}$$

where S is an arbitrary surface, which surrounds the scatterer (the crack in this case), j and k are dummy indices (the summation convention is used here) and n_j is the unit outward normal of S. In Eq. (2) the terms with superscript (1) relate to the fields in the absence of the scatterer, while terms with the superscript (2) relate to the fields in the presence of the scatterer. For the case where the scatterer is a traction free crack, Eq. (2) is simplified to

$$\delta\Gamma = -\frac{i\omega}{4P}\int_A (\sigma_{kj}^{(1)} \Delta u_k^{(2)}) n_l \, dS, \tag{3a}$$

where A is the crack area and

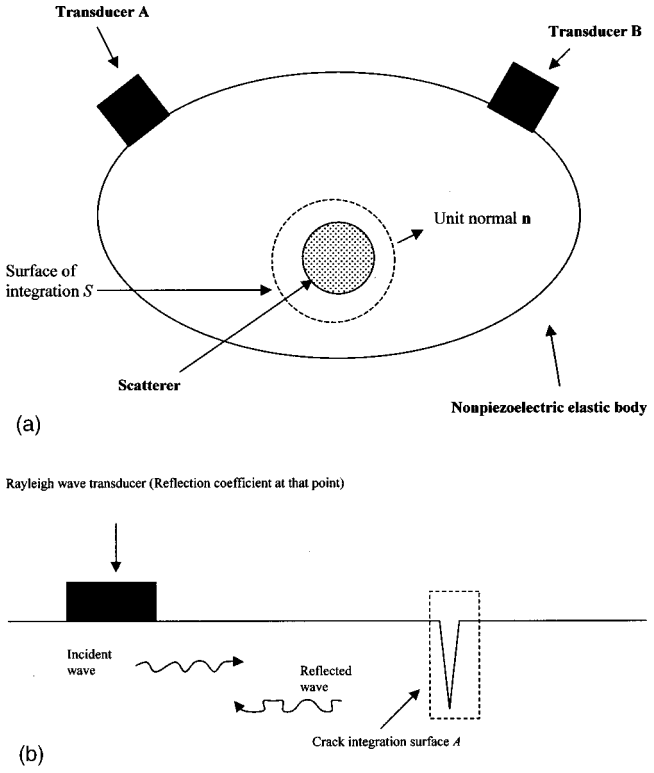

FIG. 4. (a) Auld's formula (general scattering geometry). (b) Auld's formula (backscattering case).

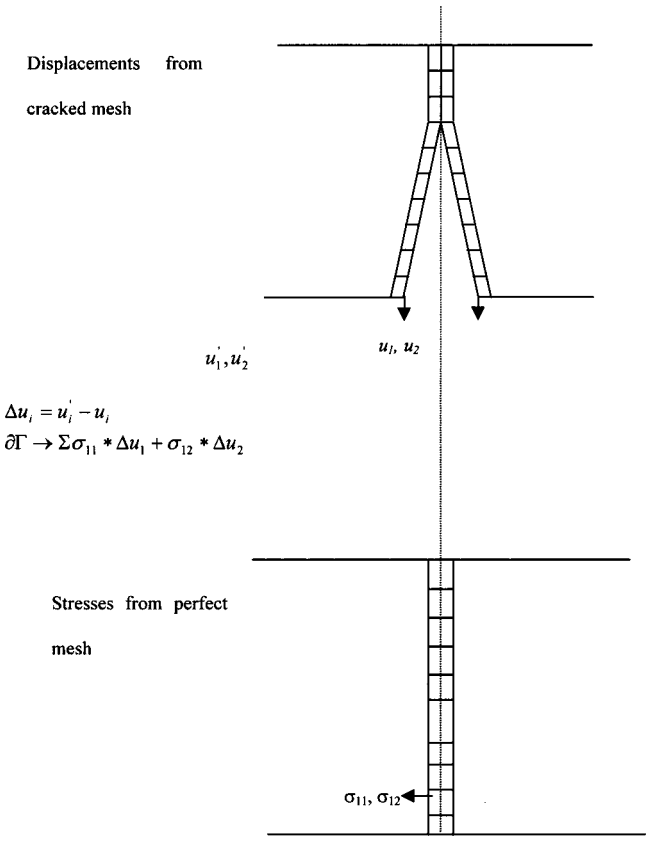

FIG. 5. Auld's formula—scheme of FEM computations.

$$\Delta u_k^{(2)} = u_k(x_2^-) - u_k(x_2^+). \tag{3b}$$

The two previous equations are used to calculate the backscattering from a surface crack at the inner radius of the cylinder.

Since the stress and displacement signals obtained from ABAQUS are transient and not time harmonic, they cannot be multiplied directly into the integrand of Eq. (3). The typical procedure[17,18] involves applying the fast Fourier transform (FFT) to the transient displacement and stress signals (the signals calculated with ABAQUS) first, then multiplying them (element by element, array multiplication and *not* vector multiplication), repeating the steps for each new value, and finally adding everything. Once the sum is obtained, it has to be multiplied by $i\omega$ (element by element again) and the resulting output is Auld's formula in the frequency domain. In addition, the inverse FFT has to be applied if a time domain result is desired. This procedure is lengthy and requires careful attention to the proper application of the FFT. In particular, zero-padding the time-domain data is absolutely necessary. Otherwise, the final signal violates causality.

An interesting alternative to the frequency-domain formulation is to adapt Eq. (3) so that it can be applied directly to time-domain signals. It is well known that the convolution in the time domain is equivalent to the multiplication in the frequency domain. In fact, many convolution programs use that property directly in their codes: they first zero-pad the data, apply the FFT, array multiply, and apply the inverse FFT to get the final outcome.[19] Equivalently, MATLAB uses a filter-based approach whereby the structures of the data are cross multiplied:

$$y(n) = f(n) * g(n) = \sum_{m=-\infty}^{\infty} f(n-m).g(m). \tag{4}$$

The advantage of using the cross multiplication, as done in MATLAB, is that much fewer operations are required (than in the alternative FFT-based formulation) and that the output is directly in the time domain. The only additional step that is required for agreement with Eq. (3) is a time differentiation, since multiplying by $i\omega$ in the frequency domain is equivalent to differentiating (with respect to time) in the time domain.

The time-domain reflection coefficient, R, is therefore calculated by using the following formula (up to a multiplicative constant):

$$R \propto \frac{d}{dt}\left(\sum_n u_i^n * \sigma_{i1}^n \right), \tag{5}$$

where n is the number of the element in consideration (for the stress tensor) and of that element's bottom node on the crack surface (for the displacement field), $*$ denotes convolution, and $i = 1,2$.

All the cracks considered in this study are radial (e.g., vertical along the 90° angle, or the y axis). Therefore, the stress tensor will always have a normal in the 0° angle direction, or the x axis (see Fig. 5). Therefore, the j index is always equal to 1.

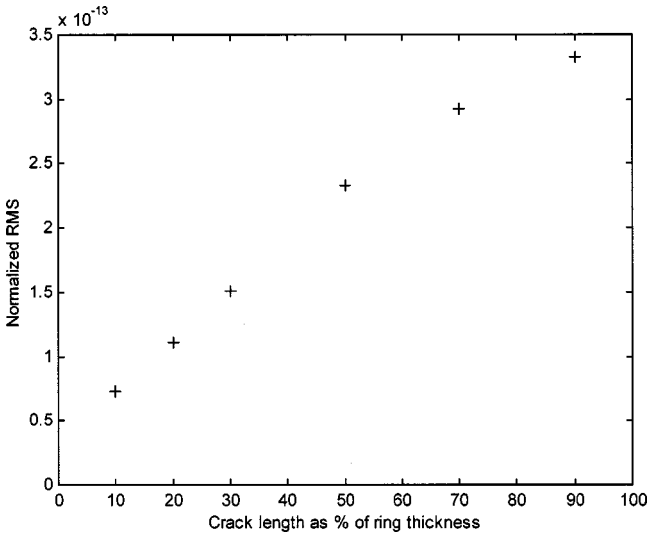

FIG. 6. Normalized RMS of FFT of Auld's reflection coefficient R versus crack depth.

IV. REFLECTION COEFFICIENT VERSUS CRACK LENGTH

Clearly, the longer the crack, the higher the overall level of the resulting reflection coefficient. One way to obtain a quantitative measure of this relationship is to plot the RMS (root-mean-square) value of the frequency spectrum of the reflection coefficient obtained via Auld's formula, for various crack lengths. That is, once the FE model is used to calculate the field around the crack, Auld's formula is then used to predict the length of the crack with this FE data. The procedure involves a series of steps.

(1) Construct a FEM model of the cylinder with a prescribed crack length.
(2) Solve for the pertinent displacement and stress fields around the crack (for the load case with a center frequency of 0.5 MHz).
(3) Obtain the time-domain (transient) reflection coefficient, R, from the procedure described in the preceding section and by applying Eq. (5), up to an arbitrary multiplicative constant.
(4) Apply the FFT to R to get its frequency spectrum.
(5) Get the RMS value of R's frequency spectrum, and normalize it with respect to the RMS value of the incident signal.
(6) Plot the normalized RMS value with respect to crack length, and repeat the entire procedure for other crack lengths.

The resulting plot is shown in Fig. 6 for six different crack lengths (10%, 20%, 30%, 50%, 70%, and 90% of cylinder wall). Figure 6 demonstrates that there is a quasilinear correlation between the crack length and the overall value of the reflection coefficient. For a perfect cylinder (crack length of 0%) there should be no backscattered energy and thus the normalized RMS should be 0. If the cylinder is completely cut (crack length of 100%) the backscattered energy should be equal to the incident energy. Figure 6 shows that the slope is steeper for crack depths smaller than 10% of the cylinder wall. The slope also tends to flatten slightly as the crack depth increases beyond 70%. Please note that mesh size (the number of elements needed to ensure convergence) of the ABAQUS model increases as the crack length decreases.

The quasilinear characteristic of the RMS plot shows that Auld's method, combined with the FEM model, gives a quantitative estimate of the crack length in a cracked steel cylinder using guided circumferential waves. Moreover, this method allows the sizing of cracks up to 300 μm even though the signal frequency is centered at 0.5 MHz (and never goes beyond 1.5 MHz). Note that a Rayleigh wave with a wavelength of 300 μm has a frequency of 9.7 MHz in steel.

V. TIME-FREQUENCY REPRESENTATIONS (TFRs) OF GUIDED WAVES

Now that a crack's length can be quantitatively measured, consider a procedure to determine the crack's location. Once again the main challenge is the dispersive and multimode nature of guided waves. For example, consider a time-domain scheme that uses arrival times to determine the unknown location of a crack on a cylinder's inner surface. Since this scheme must be based on the arrival times of a particular wave form feature, the dispersive nature of guided waves presents a large source of error. The reason for this (potential) breakdown is that the different frequencies of a dispersive wave travel with different group velocities, changing the wave's shape as it propagates. As a result, it is difficult (if not impossible) to track and identify the exact arrival time of the same feature of a propagating guided wave.

In order to alleviate this problem, changes in the frequency content of the signal need to be tracked as a function of time so that dispersion can be taken into account.

The time-frequency representation (TFR) of a signal is a quantitative measure of how a signal's frequency changes with respect to time. A TFR is obtained by dividing a time-domain signal into a series of small pieces in time; each of these pieces is windowed and then individually transformed into the frequency domain. Popular transforms include wavelets, the short time Fourier transform (STFT), and the Wigner–Ville distribution (WV). Please recall from the preceding discussion that the identification of an individual mode's arrival time is very difficult (if not impossible) from either the time-domain signal or its frequency spectrum, because the contributions from each mode in a multimode signal are not separable. However, the TFR enables the separation of the contribution of each mode, as a function of time *and* frequency simultaneously.

One problem inherent to a TFR is the time-frequency resolution limitation, that is, the impossibility to simultaneously have perfect resolution in both time and frequency. One way to increase time-frequency resolution, is through the reassignment (or reallocation) method.[20] Reassignment is not another TFR, but a way to reduce the spread of a TFR by concentrating its energy to its (the energy's) center of gravity. The reassignment method is not restricted to a specific TFR, but can be applied to any time-frequency shift invariant distribution of Cohen's class.[21] The energy density spectrum of the reassigned STFT, called the reassigned spectrogram, is

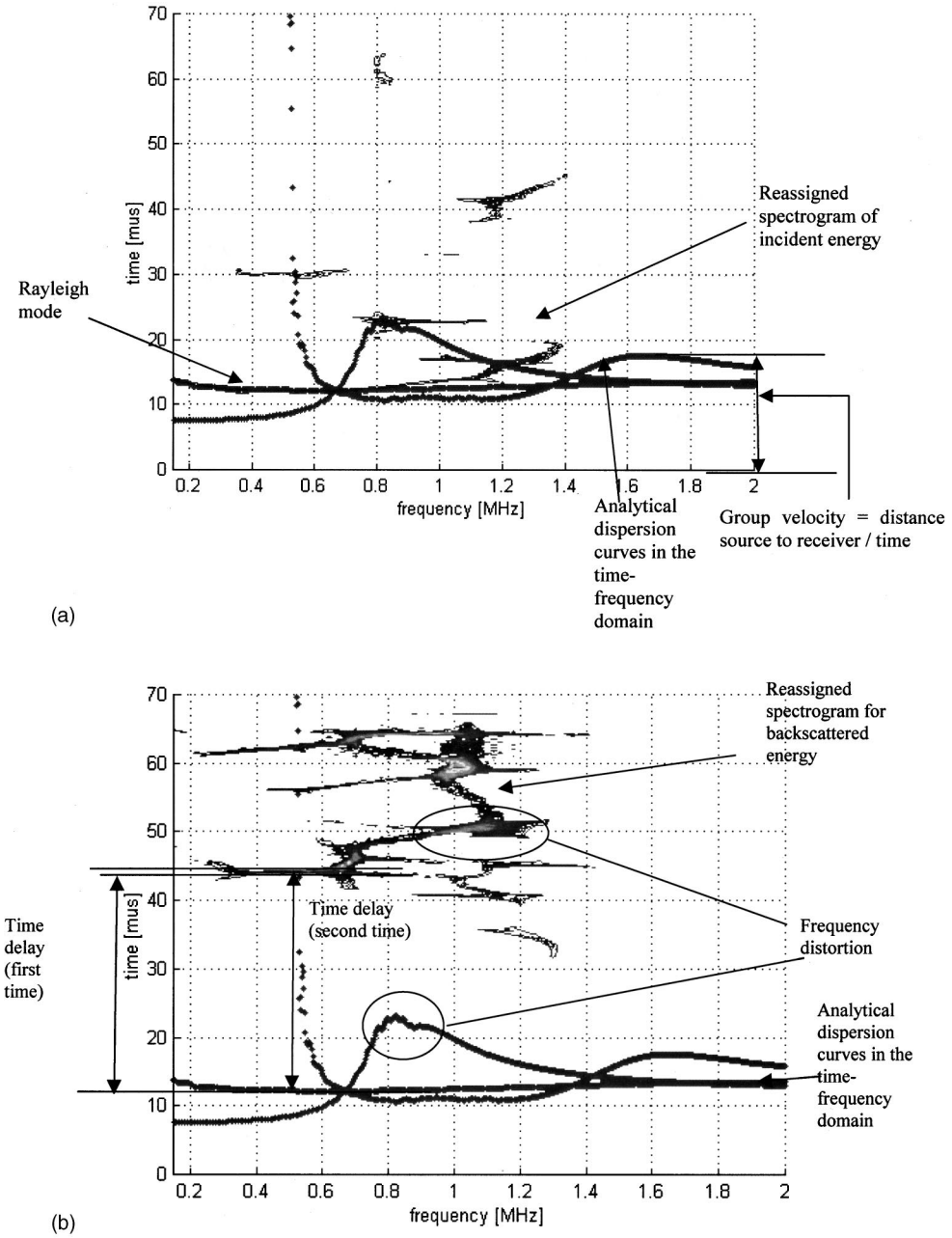

FIG. 7. (a) Comparison between the reassigned spectrogram of a FE-obtained guided circumferential wave and the analytical dispersion curves, in the time-frequency domain, of the same cylinder (both perfect). (b) Methodology to locate the crack: comparison between the reassigned spectrogram for the backscattered energy and the analytical dispersion curves in the time-frequency domain.

selected for this study, since previous work[21,22] shows that it is extremely effective in capturing the dispersive nature of guided, multimode ultrasonic signals in thin metallic plates.

Therefore, as was done in earlier studies for plates,[22] it is possible to compare analytical dispersion curves for the cylinder (calculated in the time-frequency domain) to a TFR calculated from either experimentally or numerically (FEM) generated guided circumferential wave signals. [See Fig. 7(a) for a comparison between the reassigned spectrogram of a synthetic, i.e., numerical, signal from a perfect cylinder and the analytical dispersion curves, calculated in the time-frequency domain, for that same perfect cylinder.] The ''ladder'' effect described earlier in plates[22] is clearly still present for guided circumferential waves, and although the Rayleigh mode is well represented by the TFR, the procedure breaks down beyond 0.8 MHz because the FE model's mesh is optimized for frequencies around 0.5 MHz.

One of the greatest advantages of the proposed technique is that both numerical and experimental TFRs are not limited to perfect geometries, while analytical dispersion curves (in general) have this limitation. It is thus possible to compare *in the time-frequency domain* analytically obtained dispersion curves (for a *perfect* cylinder) to a reassigned spectrogram obtained from a signal numerically calculated (or experimentally measured) in a *cracked* cylinder, using this comparison to quantify the crack's effect on these dispersion curves. *This comparison offers a systematic procedure to locate a crack that does not require the selective generation or detection of a particular mode.* Applying the reassigned spectrogram to *backscattered* ultrasonic energy and comparing it to analytical dispersion curves for the cylinder (calculated in the time-frequency domain) provides an excellent way to calculate the arrival times of specific modes (see Fig. 1 for the positioning of the source, the receiver and

the crack). A typical plot that results from the proposed procedure is given in Fig. 7(b).

From Fig. 7(b) it is possible to determine:

- which modes are affected by the crack,
- for what times and what frequencies,
- and even more importantly, by how much time is the arrival of each mode changed by the mode's interaction with the crack, for any given frequency.

This information is then used to determine the crack's location. The next section will illustrate how this information is extracted from the signals.

VI. CRACK LOCATION USING THE REASSIGNED SPECTROGRAM

This portion of the study develops FE models for two cases of the same steel cylinder, one with a crack length of 10% of the cylinder's wall (on the inner surface) and a load of center frequency of 0.5 MHz, and the second is the associated ''perfect'' cylinder (no crack). The time-domain signal backscattered from this crack is determined by subtracting the signal predicted with the cracked cylinder model from the signal of the perfect cylinder (i.e., the model without a crack), noting that each signal has the *same source and receiver locations*. The reassigned spectrogram is then applied to this backscattered signal, and this TFR is compared to the (perfect) cylinder's analytical dispersion curves (calculated, in the time versus frequency domain, for the *same source and receiver locations*). This comparison illustrates which modes are affected by the crack, as well as enabling the calculation of the time delay between the backscattered and the corresponding analytical dispersion curves [see Fig. 7(b)]. The reason for this time delay is that the backscattered signal only starts after the incident signal has propagated from the source to the receiver (as in the perfect cylinder case) and *then* to the crack *and* then back to the receiver. Therefore, the backscattered signal is zero for all times prior to the time that it takes to return to the receiver.

This time delay is given by the ratio between the group velocity of each specific mode, for a specific frequency, and twice the distance between the receiver and the crack. Note that there is a distortion in the backscattered reassigned spectrogram, when compared to the analytical dispersion curves, because the group velocity of most modes changes with frequency—this causes a change in the time delay, with frequency. As a result, the shape of the backscattered spectrogram looks slightly different from the shape of the corresponding analytical dispersion curves for the perfect cylinder [see Fig. 7(a)].

This distortion makes it difficult to identify exactly which feature of a given backscattered mode, for a specific frequency, corresponds to what feature of the analytical dispersion curve for that mode and for what frequency. For example, in Fig. 7(a), the highest peak in the second mode occurs at 0.82 MHz in the analytical dispersion curve, but finding this exact same feature in the backscattered spectrogram for the second mode is impossible since the peak is now spread over a small frequency range (1 to 1.2 MHz). Therefore, since the group velocity depends on frequency,

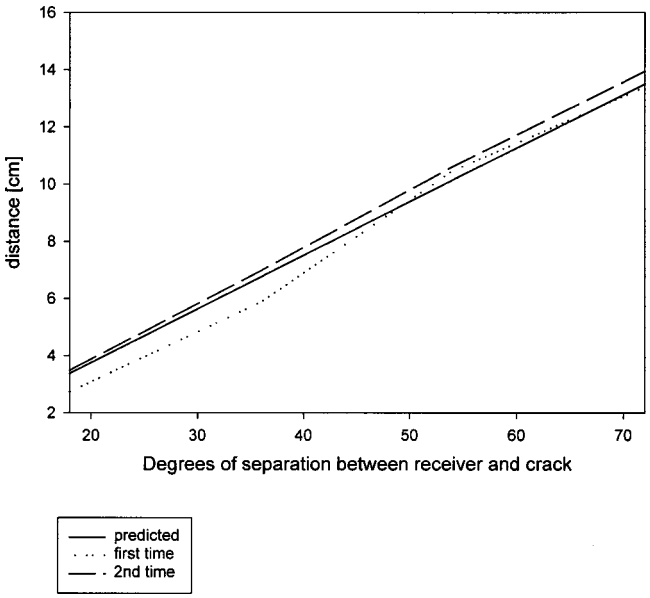

FIG. 8. Comparison between predicted distances receiver to crack (lower and upper bound) and the true distance, for the ring cracked at 10%.

the time delay between the reassigned spectrogram of a backscattered mode and its dispersion curve will also be hard to determine accurately. The only mode for which the preceding statement is not true is the Rayleigh mode, because its group velocity is constant for almost all frequencies, so the frequency distortion between the Rayleigh mode's analytical dispersion curve and its reassigned spectrogram is nearly nonexistent [beyond 0.4 MHz, shown in Fig. 7(a)]. *The time delay between the backscattered Rayleigh mode from the reassigned spectrogram and its predicted analytical arrival, times the group velocity of the Rayleigh mode, gives twice the distance between the receiver and the crack.*

Since the scattered Rayleigh mode, as calculated with the reassigned spectrogram, is not an infinitely thin line [as is clear from Figs. 7(a) and (b)], two distances are always calculated, one corresponding to the lowest bound in time (first time), and one corresponding to the upper bound in time (second time). At 0.5 MHz, the Rayleigh wave can be assumed to be almost nondispersive, thus if it reaches the receiver in a faster time, it has traveled a comparatively shorter distance. Hence the ''lower'' bound on the distance to, or location of, the flaw. Conversely the second and longer time corresponds to a longer distance traveled by the backscattered signal to the receiver. Hence the lower bound on the distance to the flaw. These distances can then be plotted against the true distance, i.e., the actual location of the crack. The comparison between those three distances is given in Fig. 8. There is very good agreement between them, even for this small (10% of wall thickness) crack.

The proposed methodology also works well in the nearfield of the crack (or source), although it is more difficult to accurately determine separation times between backscattered and analytical modes in this case; for example, the analytical modes will tend to be compressed all together toward the zero time axis if the receiver is close to the source. Since the method is based on a graphical calculation of time

delay, it is essential to have a definite separation between the analytical dispersion curves and their backscattered counterparts.

More importantly, the Rayleigh mode is not always the mode most sensitive to the crack. Indeed, in Fig. 7(b), one can see that for certain frequency ranges (for example, from 1 MHz on), the backscattered contribution from the Rayleigh mode simply vanishes. This means that for frequencies above about 1 MHz, the Rayleigh mode does not ''see'' the crack (this makes sense since the Rayleigh mode travels on the outside radius while the crack originates from the inside surface—therefore, as the frequency increases the Rayleigh mode is increasingly less likely to see the crack). Only the higher order modes (in this case the second mode) see the crack at that particular frequency (as was first shown in Valle *et al.*[4])—this is clearly visible in Fig. 7(b). Unfortunately, frequency distortion is a problem for these higher modes. This frequency distortion makes it difficult to use higher order modes to determine the location of the crack, unless one can select a frequency range with limited dispersion, so that the group velocity can be calculated accurately. Typically this frequency range exists, but it may be prohibitively high from a computational cost perspective. Please note that dispersion curves and FE signals tend to be costly for frequencies beyond 3 to 4 MHz.

This problem (the Rayleigh mode not being sensitive to cracks) only occurs for very small cracks. The reassigned spectrogram applied to time-domain signals created by a 0.5 MHz signal is clearly sufficient to locate this 300 μm crack (10% of the cylinder's thickness).

VII. SUMMARY AND CONCLUSIONS

This paper uses the FEM to model the propagation of guided circumferential waves in a cracked cylinder and presents sophisticated digital signal processing algorithms that characterize the waves' interaction with this crack. Specifically, this paper presents a technique to size the crack, and another to locate it.

For sizing the crack, a time domain analysis based on Auld's scattering formula for backscattered signals is used. By using the Auld's formula to calculate the RMS value of the frequency spectrum of the reflection coefficient for various crack lengths, it is shown that there is a quasilinear correlation between the crack depth and the overall RMS value of the reflection coefficient R. The RMS value of R increases with crack depth, and provides a quantitative means of characterizing cracks down to about 10% of the thickness of the cylinder. As a result, Auld's method combined with the FEM model gives a quantitative estimate of the crack depth from a measured signal.

To locate the crack, the reassigned spectrogram is presented as a digital signal processing algorithm that accurately captures a TFR of guided circumferential waves over a large frequency range. The reassignment method solves the time-frequency resolution problem inherent to using Fourier-based TFRs such as the spectrogram by redistributing the energy content of each mode to its center of gravity, with respect to time and frequency, and therefore clearly separates the contribution of each mode within the scattered signal. Applying the reassigned spectrogram to backscattered data, and comparing this to the analytical dispersion curves for the perfect cylinder provides an accurate measure of the time delay, per mode, between the incident signal of a perfect waveguide and its backscattered counterpart (if a crack is present). Through this time delay and the group velocity of the mode of interest at a specific frequency, the distance between the receiver and the crack can be calculated. This method can characterize cracks and notches with lengths as small as 10% of the waveguide wall. Computational power needs to be increased if even smaller sizes are of interest.

It is important to note that the results presented in this paper, both for crack sizing and crack locating, are dependent on the frequency of the input signal. Both methods (Auld's formula and the reassigned spectrogram) are applied to signals created with an input with a frequency range between 0.2 and 1.5 MHz (with most of the energy centered around 0.5 MHz) but they can detect cracks down to 300 μm—even though the wavelengths of these signals is much greater than 300 μm. Therefore, the need for high frequency signals to detect small cracks is significantly reduced by using these techniques.

Also, multiple cracks can be detected using those techniques. The reassigned spectrogram will locate them by showing a series of time delays. Auld's formula (as presented here with no restriction on the duration of the signals) can only show a combined total of damage accumulation—however, if it is used in combination with the reassigned spectrogram, the signals used in Auld's formula can be restricted to the pertinent time of flight and therefore can then characterize each crack singly, in the same fashion presented earlier in this paper.

ACKNOWLEDGMENTS

This work is supported by the Office of Naval Research M-URI Program ''Integrated Diagnostics'' (Contract No. N00014-95-1-0539). Two Amelia Earhart Fellowships from the Zonta Foundation, and support from the Deutscher Akademischer Austausch Dienst (DAAD) are also gratefully acknowledged by the first and second authors, respectively.

[1] P. B. Nagy, M. Blodgett, and M. Godis, ''Weep hole inspection by circumferential creeping waves,'' NDT & E Int. **27**, 131–142 (1994).
[2] D. E. Chimenti, ''Guided waves in plates and their use in material characterization,'' Appl. Mech. Rev. **50**, 247–284 (1997).
[3] D. N. Alleyne and P. Cawley, ''The long range detection of corrosion in pipes using lamb waves,'' Rev. Prog. Quant. Nondestr. Eval. **14**, 2073–2080 (1995).
[4] C. Valle, J. Qu, and L. J. Jacobs, ''Guided circumferential waves in layered cylinders,'' Int. J. Eng. Sci. **37**, 1369–1387 (1999).
[5] C. Valle, ''Guided circumferential waves in annular structures,'' Ph.D. thesis, Georgia Institute of Technology, Atlanta, Georgia, 1999.
[6] I. A. Viktorov, *Rayleigh and Lamb Waves* (Plenum, New York, 1967).
[7] I. A. Viktorov, ''Rayleigh-type waves on a cylindrical surface,'' J. Acoust. Soc. Am. **4**, 131–136 (1958).
[8] G. Liu and J. Qu, ''Guided circumferential waves in a circular annulus,'' J. Appl. Mech. **65**, 424–430 (1997).
[9] B. A. Auld, *Acoustic Fields and Waves in Solids*, 2nd ed. (R. E. Krieger, Melbourne, FL, 1990), Vols. 1 and 2.
[10] J. Zhu, A. H. Shah, and S. K. Datta, ''Transient response of a composite plate with delamination,'' J. Appl. Mech. **65**, 664–670 (1998).
[11] S. K. Datta, T. H. Ju, and A. H. Shah, ''Scattering of an impact wave by a crack in a composite plate,'' J. Appl. Mech. **59**, 596–603 (1992).

[12] F. Moser, L. J. Jacobs, and J. Qu, ''Modeling elastic wave propagation in wave guides with the finite element method,'' NDT & E Int. **32**, 225–234 (1999).
[13] M. J. S. Lowe, R. E. Challis, and C. W. Chan, ''The transmission of Lamb waves across adhesively bonded lap joints,'' J. Acoust. Soc. Am. **107**, 1333–1345 (2000).
[14] G. Liu and J. Qu, ''Transient wave propagation in a circular annulus subjected to transient excitation on its outer surface,'' J. Acoust. Soc. Am. **104**, 1210–1220 (1998).
[15] ABAQUS-Standard version 5.6 User's Manuals, Theory Manual, Example Problems Manual, and ABAQUS-Post Manual, 1996.
[16] B. A. Auld, ''General electromechanical reciprocity relations applied to the calculation of elastic wave scattering coefficients,'' Wave Motion **1**, 3–10 (1979).
[17] M. J. S. Lowe, P. Cawley, J-Y. Kao, and O. Diligent, ''Prediction and measurement of the reflection of the fundamental anti-symmetric Lamb wave from cracks and notches,'' Rev. Prog. Quant. Nondestructive Eval. **19**A, 193–200 (2000).
[18] M. Lowe, ''Characteristics of the reflection of lamb waves from defects in plates and pipes,'' Rev. Prog. Quant. Nondestr. Eval. **17**, 113–120 (1997).
[19] W. H. Press, B. P. Flannery, S. A. Tenkolsky, and W. T. Vetterling, *Numerical Recipes* (Cambridge University Press, Cambridge, 1988).
[20] F. Auger and P. Flandrin, ''Improving the readability of time-frequency and timescale representations by the reassignment method,'' IEEE Trans. Signal Process. **43**, 1068–1098 (1995).
[21] M. Niethammer, ''Application of time frequency representation to characterize ultrasonic signals,'' M.S. thesis, Georgia Institute of Technology, Atlanta, Georgia, 1999.
[22] M. Niethammer, L. J. Jacobs, J. Qu, and J. Jarzynski, ''Time-frequency representation of lamb waves using the reassigned spectrogram,'' J. Acoust. Soc. Am. **107**, L19–L24 (2000).